Establishment of pathology-validated immortalized patient-derived ovarian endometriosis epithelial cell line

SAOWALUK SAISOMBOON[1], NATHAKORN SRIKUMMOON[1], JATUPORN PATTANACHOT[1], PILAIWAN KLEEBKAOW[2,3], SIRIRUTHAI AMNATBUDDEE[2], RAKSAWAN DEENONPOE[3,4], PHONGSATHORN WICHIAN[3], NATRUJA SRIDAKHUN[3], THANYATHORN EAKPINITPITAYA[3], BANDIT CHUMWORATHAYI[2], WUNCHANA SEUBWAI[5], RAYNOO THANAN[1], SOMCHAI PINLAOR[6], SEIJI OKADA[7] and KULTHIDA VAETEEWOOTTACHARN[1,7,8]

[1]Department of Biochemistry and Center for Translational Medicine, Faculty of Medicine, Khon Kaen University, Khon Kaen 40002, Thailand; [2]Department of Obstetrics and Gynecology, Faculty of Medicine, Khon Kaen University, Khon Kaen 40002, Thailand; [3]Department of Pathology, Faculty of Medicine, Khon Kaen University, Khon Kaen 40002, Thailand; [4]Cholangiocarcinoma Research Institute, Khon Kaen University, Khon Kaen 40002, Thailand; [5]Department of Forensic Medicine, Faculty of Medicine, Khon Kaen University, Khon Kaen 40002, Thailand; [6]Department of Parasitology, Faculty of Medicine, Khon Kaen University, Khon Kaen 40002, Thailand; [7]Division of Hematopoiesis, Joint Research Center for Human Retrovirus Infection and Graduate School of Medical Sciences, Kumamoto University, Kumamoto 860-0811, Japan; [8]Northeast Laboratory Animal Center, Khon Kaen University, Khon Kaen 40002, Thailand

Received March 11, 2026; Accepted August 28, 2026

DOI: 10.3892/br.2026.2206

Abstract. Endometriosis is a heterogeneous gynecological disorder for which experimental model development is often limited by diagnostic ambiguity and the restricted lifespan of primary epithelial cultures. Although immortalization strategies enable long-term expansion of patient-derived cells, concerns remain regarding the preservation of disease-specific biological characteristics and the risk of model misclassification in the absence of definitive pathological confirmation. In the present study, immortalized ovarian epithelial cell lines from clinically suspected ovarian cystic lesions representing endometriosis were established and it was evaluated whether disease-intrinsic biological features were preserved following immortalization, as determined by definitive histopathological stratification. Primary epithelial cells were isolated from two ovarian cystic lesions and immortalized via lentiviral co-expression of constitutively active cyclin-dependent kinase 4 ($CDK4^{R24C}$), cyclin D1 and human telomerase reverse transcriptase. One lesion was subsequently identified as an ovarian endometrioma, and the other as a mature cystic teratoma, in postoperative histopathology. The endometriosis-derived immortalized epithelial line iEn1 exhibited sustained proliferative capacity (Cell Counting Kit-8 assay), maintained epithelial lineage characteristics (western blotting for pan-cytokeratin, β-catenin and claudin-1), and retained a stable 46,XX karyotype. These cells demonstrated epithelial-mesenchymal plasticity evidenced by co-expression of epithelial markers with vimentin and N-cadherin, and formed microscopic glandular structures resembling endometriosis-like lesions in an estrogen-supplemented xenograft model. However, immunohistochemistry revealed that estrogen receptor β and interleukin-6, both frequently implicated in endometriosis-associated inflammation, were not detected in either the original tissue or the xenografted lesions, indicating that this particular inflammatory phenotype is not intrinsic to this model. By contrast, the teratoma-derived line iEn2 displayed marked chromosomal instability and phenotypic heterogeneity, demonstrated by karyotyping, consistent with its germ cell origin. Thus, immortalization alone does not determine the biological validity of patient-derived cellular models; rather, accurate interpretation requires integration with definitive histopathological classification. The present study established a pathology-validated immortalized epithelial model of ovarian endometriosis and highlighted the importance of pathology-integrated frameworks for improving experimental rigor in disease modeling.

Correspondence to: Dr Kulthida Vaeteewoottacharn, Department of Biochemistry and Center for Translational Medicine, Faculty of Medicine, Khon Kaen University, 123 Mittapap Road, Khon Kaen 40002, Thailand
E-mail: kulthidava@kku.ac.th

Key words: endometriosis, patient-derived cell lines, immortalized epithelial cells, ovarian endometrioma, epithelial-mesenchymal plasticity, cystic teratoma

Introduction

Endometriosis is a common chronic gynecological disorder affecting women of reproductive age, characterized by the

presence of endometrial-like glands and stroma outside the uterine cavity (1). Clinically, the disease is associated with pelvic pain, dysmenorrhea, dyspareunia and infertility, imposing a substantial burden on patients' quality of life and healthcare systems worldwide (1). Although histologically benign, endometriosis exhibits several biological properties commonly seen in neoplastic processes, including enhanced proliferative capacity, resistance to apoptosis, invasive behavior and altered immune interactions (2). These features suggest that endometriosis is a complex disease involving dysregulated cellular behavior rather than simple ectopic implantation of endometrial tissue.

Increasing evidence indicates that epithelial cells play a central role in the pathogenesis and persistence of endometriotic lesions. In particular, endometriotic epithelial cells frequently display epithelial-mesenchymal plasticity, a hybrid cellular state in which they partially acquire mesenchymal characteristics while maintaining the epithelial identity (3). This plasticity is believed to contribute to lesion implantation, invasion and survival in ectopic environments (3,4). Therefore, understanding the molecular mechanisms underlying epithelial cell behavior in endometriosis is an important step toward elucidating disease pathogenesis and identifying potential therapeutic targets.

The experimental investigation of endometriosis biology has been hindered by the limited availability of reliable cellular models (5). Primary epithelial cells isolated from endometriotic lesions retain patient-specific biological characteristics and therefore act as valuable experimental material. However, these primary cultures undergo replicative senescence after a limited number of passages, restricting their utility for long-term mechanistic studies (6). Immortalization strategies can overcome this limitation by extending cellular lifespan; however, concerns regarding potential alterations in cellular phenotype, genomic stability or biological behavior following immortalization remain (6,7). Therefore, establishing immortalized epithelial cell models that maintain disease-relevant biological properties remains a critical challenge in endometriosis research (5).

Several approaches, such as transfection with human telomerase reverse transcriptase (hTERT) alone or with human papillomavirus type 16 E6-E7-hTERT, have been developed to extend the lifespan of human epithelial cells while minimizing oncogenic transformation (6,7). The co-expression of constitutively active cyclin-dependent kinase 4 ($CDK4^{R24C}$), cyclin D1 and hTERT enables bypass of the $p16^{INK4a}$-Rb cell-cycle checkpoint and stabilizes telomere length, thereby promoting sustained proliferation (8,9). This strategy can be used to immortalize epithelial cells while preserving their differentiation potential and lineage characteristics, making it a promising approach for developing long-term experimental cell models (10).

Another challenge in developing patient-derived models of endometriosis is the diagnostic complexity of ovarian cystic lesions. Ovarian endometriomas may overlap clinically and radiologically with other ovarian pathologies, including mature cystic teratomas and other benign tumors (11,12). Consequently, epithelial cells isolated from ovarian cystic lesions initially suspected to represent endometriosis may originate from distinct pathological entities if definitive histopathological confirmation is not considered. This diagnostic overlap highlights the importance of careful pathological evaluation when interpreting the biological characteristics of patient-derived cell models.

The present study aimed to establish a disease-relevant immortalized epithelial cell model of endometriosis by integrating postoperative histopathological diagnosis with experimental characterization and to examine how pathological classification influences the interpretation of patient-derived cellular models. Immortalized epithelial cell lines from ovarian cystic lesions clinically suspected to represent endometriosis were established using lentiviral-mediated co-expression of $CDK4^{R24C}$, cyclin D1 and hTERT. The proliferative capacity, epithelial lineage markers and genomic stability of the resulting immortalized cell lines were then characterized and their biological properties were evaluated *in vitro* and *in vivo*.

Materials and methods

Patient background. En1: A 33-year-old woman with a 5-year history of infertility and dysmenorrhea underwent transvaginal ultrasonography, which revealed an 8.0x5.1 cm multiloculated hypoechoic cyst in the left ovary and focal uterine adenomyosis. A preoperative diagnosis of left ovarian endometrioma with adenomyosis was made. Serum tumor marker levels were not assessed. The patient underwent laparoscopic left ovarian cystectomy in March 2023. Intraoperative findings included a nodular enlarged uterus (10x8 cm), a multiloculated ovarian cyst containing chocolate-like serous fluid and pelvic adhesions. Histopathological examination confirmed the ovarian endometrioma.

En2: A 42-year-old woman with morbid obesity presented with hypermenorrhea and severe dysmenorrhea. The patient had previously received hormonal therapy, including dienogest and a gonadotropin-releasing hormone agonist, albeit without notable symptom improvement. Ultrasonography revealed a globular uterus (10.9x6.1 cm), a 6.7x6.6 cm hypoechoic cyst with incomplete septation in the left adnexa and a 5.3x7.1 cm hypoechoic cyst in the right ovary. Serum tumor markers were not detected. The clinical diagnosis was adenomyosis with a right ovarian endometrioma and a left ovarian tumor. The patient underwent laparoscopic right ovarian cystectomy and left salpingo-oophorectomy in August 2023. Intraoperative findings included bilateral ovarian cysts containing sebaceous material and hair. Histopathology confirmed a mature cystic teratoma in both ovaries.

Patient tissues. Surgically resected ovarian tissues were obtained from the operating room of Srinagarind Hospital, Faculty of Medicine, Khon Kaen University (Khon Kaen, Thailand). Immediately after resection, the specimens were immersed in Dulbecco's modified Eagle's medium-high glucose (DMEM-HG) supplemented with 10% fetal bovine serum (FBS) and 1X antibiotic-antimycotic solution (all from Gibco; Thermo Fisher Scientific) and transported on ice to the cell culture facility.

Tissues were sectioned into 2-5 mm fragments and divided into two portions, one for cryopreservation and one for primary cell isolation. The study was approved by the Human Research

Ethics Committee of Khon Kaen University (approval nos. HE661409 and HE681046) and was conducted in accordance with The Declaration of Helsinki. Written informed consent was obtained from all participants. Additional leftover formalin-fixed, paraffin-embedded tissue and primary cell culture material from patients with endometriosis from another project (approval no. HE651590) were used in the present study for cell line establishment and for histological and immunohistochemical comparison.

Isolation and expansion of primary cell lines. Resected tissues were mechanically minced using a surgical blade and partially digested with trypsin-EDTA at 37˚C for 2-3 min. Dissociated cells were plated in DMEM-HG supplemented with 10% FBS and 1X antibiotic-antimycotic. Cells were cultured at 37˚C in a humidified atmosphere containing 5% CO_2. Primary cultures were expanded and monitored to achieve a homogeneous population characterized by fibroblast-like, spindle-shaped morphology prior to immortalization.

Lentiviral construction and transduction. Immortalized cell lines were generated via lentivirus-mediated gene transfer. Lentiviral particles encoding $CDK4^{R24C}$, cyclin D1 and hTERT (CSII-CMV vectors; Invitrogen; Carlsbad, CA) were produced in 293T packaging cells using a second-generation packaging system with Lipofectamine® 2000 (Invitrogen; Thermo Fisher Scientific, Inc.), as described previously (10,13). Briefly, 293T cells were co-transfected with a total of 4 μg plasmid DNA per well consisting of CSII-CMV-$CDK4^{R24C}$ (0.6 μg), CSII-CMV-Cyclin D1 (0.6 μg), CSII-CMV-TERT (0.6 μg), CSII-CMV-Puro (0.2 μg), pCAG-HIVgp (1 μg) and pCMV-VSV-G-RSV-Rev (1 μg). Transfection was performed at 37˚C in a humidified atmosphere containing 5% CO_2 for 72 h. Viral supernatants were collected at 48 and 72 h post-transfection and filtered through a 0.45 μm syringe filter (Sartorius Stedim Biotech; Sartorius AG).

Primary En1 (passage 8) and En2 (passage 7) cells were transduced with viral supernatants at a 1:10 dilution in the presence of 8 μg/ml polybrene for 48 h, and selected using 2 μg/ml puromycin (cat. no. 61-385-RA; Corning, Inc.) for three consecutive passages to establish immortalized cell lines (iEn1 and iEn2). Passage numbering of immortalized lines was restarted after viral transduction.

Karyotyping analysis. Once stable in culture, iEn1 (passage 22) and iEn2 (passage 25) cells were subjected to cytogenetic analysis. The cells were treated with 1 μg/ml colcemid (KaryoMAX™ Colcemid™ Solution; Gibco; Thermo Fisher Scientific, Inc.) at 37˚C for 15 min to arrest them in metaphase, followed by hypotonic KCl treatment with 0.075 M KCl at 37˚C for 15 min and fixation with freshly prepared methanol:acetic acid (3:1, v/v). Methanol and acetic acid were stored at room temperature, and the freshly prepared fixative was pre-chilled at -20˚C before use. For cell fixation, 1 ml pre-chilled fixative was added dropwise to the cell sample with gentle mixing for 3 min, followed by the addition of 4 ml fixative with vortex mixing for 2 min at room temperature. The sample was then centrifuged at 3,000 x g at 25˚C for 5 min. The fixation and centrifugation steps were repeated twice, with the fixative added directly without dropwise addition. Centrifugation was performed after each fixation step. Giemsa-Trypsin-Giemsa banding was performed for chromosome visualization. Chromosome slides were treated with trypsin (2 mg/ml) for 3 sec, rinsed in phosphate-buffered saline, stained with Giemsa for 7 min at room temperature, and rinsed with tap water.

Metaphase spreads were analyzed using the GenASIs Bandview software version 8.4.1 (Applied Spectral Imaging) with an Olympus BX63 microscope (Olympus Corporation) and Neon karyotyping software version 6.3.16.3 (MetaSystems) with a Zeiss AX10 microscope (Carl Zeiss AG). The karyotypes of the endometriosis cells were analyzed by two cytogeneticists. A total of 40 metaphases (iEn1) and 39 metaphases (iEn2) were analyzed at 300-400 band resolution to determine modal chromosome number and structural abnormalities.

DNA extraction and short tandem repeat (STR) analysis. DNA was extracted from iEn1 and iEn2 cells using the QIAamp® DNA mini kit (QIAGEN GmbH). Following the manufacturer's instructions, all diluted DNA samples in the concentration range of 0.5-1.0 ng/μl were amplified by multiplex PCR with a commercial VeriFiler™ Plus PCR amplification kit (Thermo Fisher Scientific) on a ProFlex™ PCR System (Applied Biosystems; Thermo Fisher Scientific) under the following thermal cycling conditions: 95˚C for 1 min; 2 cycles at 96˚C for 10 sec and 62˚C for 90 sec; 27 cycles at 96˚C for 10 sec and 59˚C for 90 sec; 60˚C for 5 min; 4˚C until the next step. The kit contained 23 autosomal microsatellites, namely Penta D, Penta E, D18S51, D16S539, D3S1358, D2S1338, TPOX, FGA, D1S1656, D10S1248, D5S818, D7S820, D13S317, CSF1PO, D22S1045, D6S1043, TH01, D2S441, D8S1179, vWA, D19S433, D12S391 and D21S11, along with Y indel and sex-determining loci (Amelogenin). The amplified products were separated and visualized by capillary electrophoresis using a Genetic Analyzer (Applied Biosystems 3500 Series; Thermo Fisher Scientific, Inc.). The capillary electrophoresis data were analyzed using the GeneMapper ID-X version 1.4 software (Applied Biosystems; Thermo Fisher Scientific, Inc.).

Cell proliferation assay and β-estradiol treatment. Cells were seeded at $3x10^3$ cells per well into 96-well plates, and proliferation was assessed using the SuperKine™ Maximum Sensitivity Cell Counting Kit-8 (CCK-8; Abbkine) according to the manufacturer's instructions. At the indicated time points, the CCK-8 reagent was added, incubated for 2 h at 37˚C, and absorbance at 450 nm (OD_{450}) was measured using a microplate reader (EZ Read 2000; Biochrom, Ltd.). The OD_{450} value at 6 h after plating was designated as day 0. All experiments were performed in triplicate. Primary cells (En1 and En2) at passages 10-15 and iEn cells at passages 20-25 were used for growth comparisons.

For β-estradiol treatment, cells were plated at $3x10^3$ cells per well into 96-well plates overnight. Cells were then treated with β-estradiol at concentrations of 0, 2 and 200 nM for 1, 2 and 3 days. At the indicated time points, cell proliferation was evaluated using the CCK-8 assay.

Western blot analysis. Cells were lysed in RIPA buffer (50 mM Tris-HCl pH 7.4, 150 mM NaCl, 1% NP-40, 1% Na-deoxycholate, 0.1% SDS), and protein concentration was

determined using Bradford reagent (Bio-Rad Laboratories, Inc.). A total of 10-20 μg of protein was separated by 10-15% SDS-PAGE and transferred to PVDF membranes (MilliporeSigma). Membranes were blocked with 3% bovine serum albumin (HiMedia Laboratories, LLC) in Tris-buffered saline containing 0.1% Tween 20 (TBST) and incubated overnight at 4˚C with primary antibodies (1:1,000). After washing with TBST, membranes were incubated with HRP-conjugated secondary antibodies (1:2,000) for 1 h at room temperature and developed using Immobilon Forte HRP substrate (MilliporeSigma). Signals were detected using an ImageQuant LAS 600 system (GE Healthcare). Band intensities were quantified using ImageJ software (version 1.53k; National Institutes of Health).

The primary antibodies included anti-CDK4 (cat. no. 11026-1-AP) and anti-TERT (cat. no. 27586-1-AP) (Proteintech Group, Inc.), anti-cyclin D1 (92G2; cat. no. 2978), anti-β-catenin (D10A8; cat. no. 8480), anti-claudin-1 (D5H1D; cat. no. 13255), anti-E-cadherin (24E10; cat. no. 3195), anti-N-cadherin (cat. no. 4061), anti-vimentin (D21H3; cat. no. 5741), anti-zonula occludens-1 (ZO-1; D7D12; cat. no. 8193) (Cell Signaling Technology, Inc.), anti-pan-cytokeratin (AE-1/AE-3; cat. no. NBP2-29429) (Novus Biologicals, LLC) and anti-GAPDH (6C5; cat. no. MAB374) (Sigma-Aldrich; Merck KGaA). The secondary antibodies included HRP-linked goat anti-rabbit IgG (cat. no. 7074) and HRP-linked horse anti-mouse IgG (cat. no. 7076) (Cell Signaling Technology, Inc.).

RNA extraction and reverse transcription-quantitative PCR (RT-qPCR). Total RNA was extracted from cells using TRIzol® reagent (Invitrogen; Thermo Fisher Scientific) according to the manufacturer's protocol. RT was performed using an Applied Biosystems™ High-Capacity cDNA Reverse Transcription Kit (Applied Biosystems; Thermo Fisher Scientific, Inc.) under the following temperature protocol: 25˚C for 10 min, 37˚C for 120 min and 85˚C for 5 min. RT-qPCR was performed on a LightCycler® 480 system (Roche Diagnostics GmbH) using 20 ng of cDNA, 1 μM each of forward and reverse primers and SYBR Green I master mix (Roche Diagnostics GmbH). The thermocycling conditions were as follows: Pre-incubation at 95˚C for 5 min; followed by 40 cycles of denaturation at 95˚C for 10 sec, annealing at 60˚C for 10 sec and extension at 72˚C for 3 sec. A melting curve analysis was subsequently performed (95˚C for 10 sec, 60˚C for 10 sec and continuous heating to 97˚C). *ACTB* was used as the internal reference gene. Relative expression levels were calculated using the $2^{-\Delta\Delta Cq}$ method (14). The primer sequences were as follows: *ACTB* forward (F), 5'-GGCTGTGCTATCCCTGTACG-3' and reverse (R), 5'-AGGTAGTCAGTCAGGTCCCG-3'; *COX-2* F, 5'-CGCTCAGCCATACAGCAAAT-3' and R, 5'-ATTCCG GTGTTGAGCAGTTT-3'; and *IL-6* F, 5'-AGACAGCCACTC ACCTCTTCAG-3' and R, 5'-TTCTGCCAGTGCCTCTTT GC-3'.

H&E and immunohistochemical staining. The original patient tissues and xenograft lesions were fixed in 10% formalin at 4˚C for 24 h and embedded in paraffin. Formalin-fixed paraffin-embedded tissues were sectioned at a 3 μm thickness and stained with hematoxylin at room temperature for 3-5 min, followed by eosin for 1-2 min. Immunohistochemical staining was performed as follows: Sections were deparaffinized with xylene and rehydrated through graded alcohol series. Antigen retrieval was performed using 1X Tris-EDTA buffer, pH 8.0 with autoclaving at 121˚C for 1 min. Subsequently, endogenous peroxidase activity was blocked with 0.3% H_2O_2 in methanol for 30 min at room temperature. The sections were then blocked with 1% bovine serum albumin for 1 h at room temperature to prevent non-specific binding. Sections were subsequently incubated overnight at 4˚C with the following primary antibodies: 0.3 μg/ml anti-CD10 (56C6; cat. no. 110M-18), 0.06 μg/ml anti-cytokeratin (CK)-7 (OV-TL12/30; cat. no. 307M-96), 0.15 μg/ml anti-CK-20 (Ks20.8; cat. no. 320M-16) (Cell Marque; MilliporeSigma), 1 μg/ml anti-estrogen receptor (ER)α (SP1; cat. no. 790-4324; Roche Diagnostics GmbH), 0.9 μg/ml anti-ERβ (cat. no. 14007-1-AP; Proteintech Group, Inc.), 0.2 μg/ml anti-interleukin (IL)-6 (cat. no. A0286; ABclonal Biotech Co., Ltd.), 1 μg/ml anti-progesterone receptor (PR; 1E2; cat. no. 790-4296; Roche Diagnostics GmbH) and 0.09 μg/ml anti-Ki67 (MIB-1; cat. no. M7240; Dako; Agilent Technologies, Inc.). The EnVision+ system-HRP-conjugated polymer-anti-rabbit (cat. no. K4003) and -anti-mouse (cat. no. K4001) antibodies (ready-to-use; Dako; Agilent Technologies, Inc.) were then incubated for 1 h at room temperature. Immunoreactivity was visualized using 3'3-diaminobenzidine tetrahydrochloride hydrate (cat. no. D5637; Sigma-Aldrich; Merck KGaA) as the chromogen. Sections were counterstained with hematoxylin for 30 sec at room temperature, dehydrated, and mounted. Histopathological comparisons between original and transplanted tissues were evaluated by a pathologist. Images were captured using a Zeiss Axio microscope (Carl Zeiss Ltd.).

Ovariectomy, estradiol treatment and xenograft mouse model. Female BALB/c Rag-2/Jak3 double-deficient (BRJ) mice (6- to 8-week-old; body weight, 17-20 g) were surgically ovariectomized. β-Estradiol-3-benzoate (0.15 μg; cat. no. E8515; MilliporeSigma), dissolved in sesame oil (cat. no. S3547; Sigma-Aldrich; Merck KGaA), was administered starting on day 4 post-ovariectomy, and the procedure was repeated every 4 days for 20 days. On day 4, six mice were randomly divided into three groups (n=2/group): i) Control; ii) $5x10^5$ iEn1 cells; and iii) $1x10^6$ iEn1 cells. Cells (passage 25) were suspended in DMEM-HG containing 10% FBS and administered via intraperitoneal injection. The control group served as a negative control and received no injection. On day 20, mice were sacrificed, and peritoneal tissues were collected for histological evaluation.

Mice were monitored in the animal research facility according to institutional guidelines. All procedures were approved by the Institutional Animal Care and Use Committee of Khon Kaen University (approval no. IACUC-KKU14/68), and the study was conducted in accordance with the ARRIVE 2.0 guidelines where applicable. Mice were housed in a strictly controlled environment at 23±2˚C with 30-60% humidity, 10-15 air changes per hour, with ambient noise levels kept below 85 dB, under a 12/12-h light/dark cycle with light intensity of 350-400 lux. Food and water were provided *ad libitum*. Health and behavior were monitored daily by the research team and attending veterinarian to evaluate humane endpoints, defined

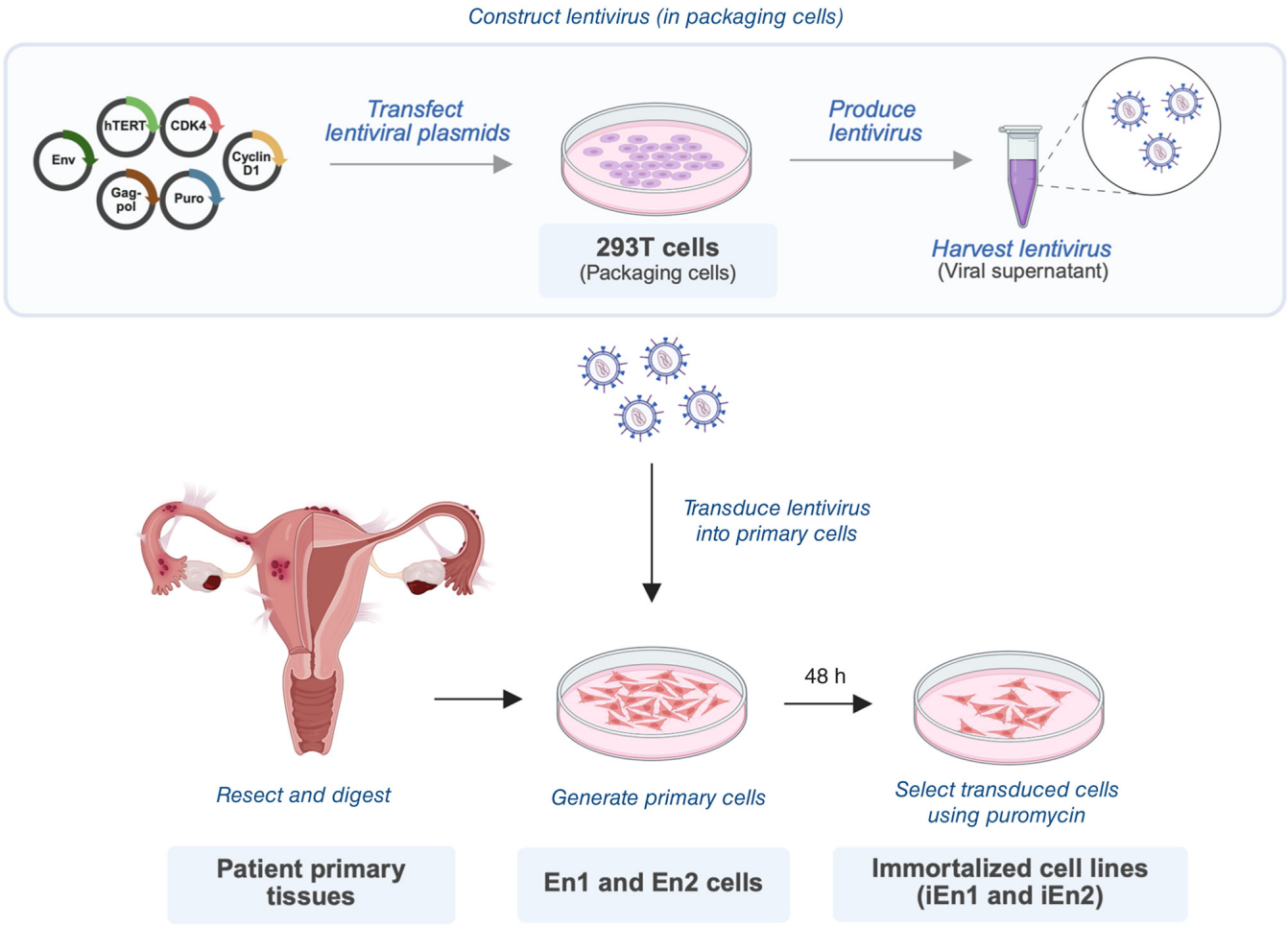

Figure 1. Experimental workflow for establishment and immortalization of patient-derived ovarian epithelial cell lines. Schematic representation of primary cell isolation and immortalization strategy. Ovarian cystic lesions from patients clinically suspected of having endometriosis were processed for primary epithelial cell culture (En1 and En2). Cells were immortalized via lentiviral co-expression of $CDK4^{R24C}$, cyclin D1 and hTERT, generating immortalized lines (iEn1 and iEn2). Definitive postoperative histopathology was subsequently used to stratify cell lines according to tissue origin. CDK4, cyclin-dependent kinase 4; hTERT, human telomerase reverse transcriptase.

as loss of appetite, severe weight loss (>20% of initial body weight) or signs of pain-associated behavior. At the end of the experiment, mice were anesthetized using 3-4% inhaled isoflurane, and anesthesia was confirmed by absence of the pedal reflex. Intracardiac blood collection (0.5-1.0 ml) was performed via percutaneous needle puncture, followed by cardiac arrest. Death was verified by the absence of respiration, heartbeat and corneal reflex, prior to peritoneal tissue collection.

Statistical analysis. Statistical analyses were performed using GraphPad Prism version 10.0.5 (GraphPad; Dotmatics). Data are presented as the mean ± SD. Differences between two groups were assessed using an unpaired two-tailed Student's t-test. Differences among multiple treatment groups were analyzed using one-way ANOVA followed by Tukey's post hoc test. $P<0.05$ was considered to indicate a statistically significant difference.

Results

Establishment and immortalization of patient-derived ovarian epithelial cells. Primary epithelial cell cultures were successfully established from ovarian cystic lesions that were clinically suspected to represent endometriosis. The primary cultures, designated En1 and En2, exhibited an elongated, fibroblast-like morphology, consistent with the previously reported features of endometriotic epithelial cells (15).

To overcome replicative senescence and enable long-term experimental applications (6,7), both primary cultures were immortalized through infection with lentiviruses co-expressing $CDK4^{R24C}$, cyclin D1 and hTERT. This strategy promotes bypass of the $p16^{INK4a}$-RB checkpoint and stabilizes telomere length, thereby supporting the sustained proliferation of epithelial cells (8-10). The overall experimental workflow for establishing immortalized cell lines is illustrated in Fig. 1.

Following viral transduction and puromycin selection, stable immortalized cell lines were obtained from both primary cultures and designated iEn1 and iEn2. Both immortalized lines retained a fibroblast-like morphology comparable to that of their parental cultures, without overt morphological transformation (Fig. 2A).

Cell proliferation analysis using the CCK-8 assay demonstrated that the immortalized cells exhibited sustained proliferative capacity compared with that of the

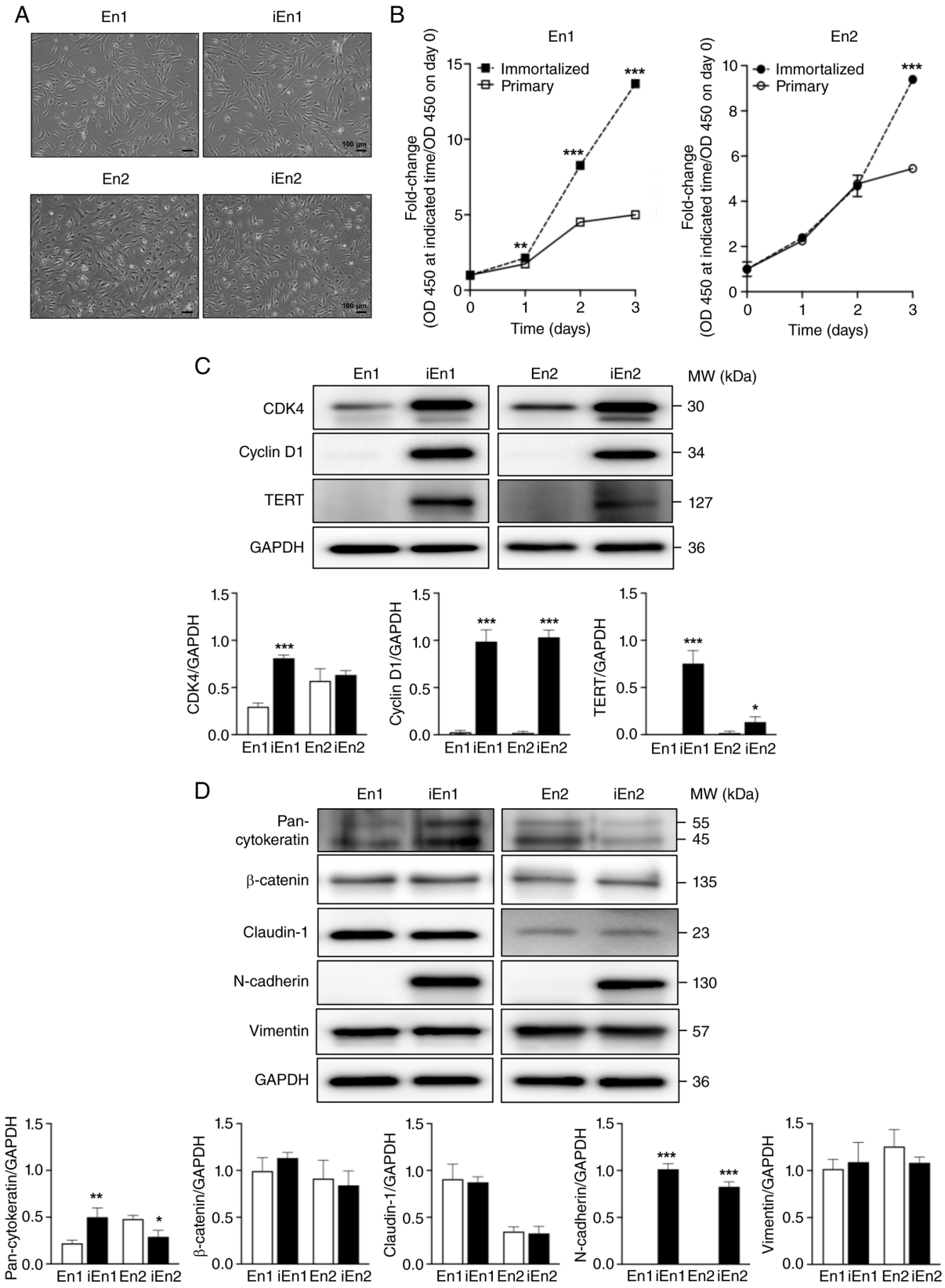

Figure 2. Morphological, proliferative and molecular characterization of primary and immortalized ovarian epithelial cells. (A) Representative phase-contrast micrographs of primary cells (En1, passage 15; and En2, passage 14) and the corresponding immortalized lines (iEn1, passage 20; and iEn2, passage 20), demonstrating fibroblast-like morphology following immortalization. All cultures were imaged at 70-80% confluence. Scale bar, 100 μm. (B) Cell proliferation assessed by the Cell Counting Kit-8 assay. Cell growth is expressed as fold change relative to day 0. Data are presented as the mean ± SD from three independent experiments. Statistical comparisons were performed between immortalized and primary cells at the indicated time points (**P<0.01 and ***P<0.001). Western blot analysis of (C) cell cycle regulators (CDK4, cyclin D1 and TERT) and (D) epithelial-mesenchymal markers (pan-cytokeratin, β-catenin, claudin-1, N-cadherin and vimentin). GAPDH was used as the loading control. The molecular weight markers are indicated. Intensities of protein bands were normalized to that of GAPDH from three independent experiments. Data are presented as the mean ± SD. The statistical comparison between primary (En) and immortalized (iEn) cell lines are indicated (*P<0.05, **P<0.01 and ***P<0.001). CDK4, cyclin-dependent kinase 4; TERT, telomerase reverse transcriptase; MW, molecular weight; OD, optical density.

Table I. Short tandem repeat analysis of patient endometriosis tissues and iEn cell lines.

	En1		En2	
Locus	Patient tissue	iEn1 cells	Patient tissue	iEn2 cells
D3S1358	17, 18	17, 18	16, 17	16, 17
vWA	14, 18	14, 18	16, 17	16, 17
D16S539	11	11	10	10
CSF1PO	11, 12	11, 12	9, 13	9, 13
D6S1043	11, 18	11, 18	19, 20	19, 20
AMEL	X	X	X	X
D8S1179	10, 12	10, 12	15	15
D21S11	30	30	30, 32.2	30, 32.2
D18S51	16, 21	16, 21	14, 18	14, 18
D5S818	12	12	9, 13	9, 13
D2S441	11, 11.3	11, 11.3	10, 14	10, 14
D19S433	14, 14.2	14, 14.2	15, 15.2	15, 15.2
FGA[a]	22, 24	23, 24	21	21
D10S1248	13, 15	13, 15	13, 16	13, 16
D22S1045	15, 17	15, 17	17, 18	17, 18
D1S1656	11, 15	11, 15	14, 17	14, 17
D13S317	8, 9	8, 9	8, 11	8, 11
D7S820	10	10	10, 11	10, 11
Penta E	10, 19	10, 19	11, 17	11, 17
Penta D	9, 13	9, 13	9, 13	9, 13
TH01	6, 9	6, 9	9	9
D12S391	18, 21	18, 21	19, 22	19, 22
D2S1338	19, 25	19, 25	19, 24	19, 24
TPOX	10, 11	10, 11	8	8

[a]A single-allele discordance was observed at the FGA locus between En1 patient tissue and iEn1 cells (22,24 vs. 23,24). Overall concordance exceeded the ≥80% threshold conventionally applied for cell line authentication (ANSI/ATCC ASN-0002-2022), consistent with shared patient origin.

corresponding primary cultures, confirming successful immortalization (Fig. 2B). Consistent with this observation, western blot analysis demonstrated increased expression of CDK4, cyclin D1 and TERT in immortalized cells compared with that observed in primary cultures (Fig. 2C), confirming the effective implementation of the immortalization strategy.

Both immortalized cell lines expressed pan-cytokeratin, β-catenin and claudin-1, indicating the preservation of epithelial lineage characteristics. In addition, the expression of vimentin and N-cadherin (Fig. 2D), together with the lack of ZO-1 and E-cadherin expression in both primary and immortalized cells (data not shown), suggested the presence of epithelial-mesenchymal plasticity within the immortalized epithelial populations.

Definitive postoperative histopathological examination revealed that the two primary lesions represented distinct pathological entities. The En1 culture originated from an ovarian endometrioma, whereas the En2 culture was classified as a mature cystic teratoma. These findings enabled the subsequent biological interpretation of immortalized cell lines according to their confirmed pathological origin.

To confirm that the immortalized cell lines authentically originated from their respective patient tissues and to exclude the possibility of cross-contamination or misidentification, STR profiling was performed on genomic DNA from the original tissues (En1 and En2) and the corresponding immortalized lines (iEn1 and iEn2) (Table I). Allelic profiles were concordant between each patient's tissue and the corresponding immortalized cell line across most loci examined, confirming the patient-specific origin of iEn1 and iEn2.

Cytogenetic profiling reveals pathology-associated genomic differences. To evaluate genomic stability following immortalization, cytogenetic analyses were performed using G-banded karyotyping. The immortalized endometriosis-derived epithelial cells (iEn1) exhibited a normal female karyotype (46,XX) across the analyzed metaphases, indicating chromosomal stability after immortalization (Figs. 3A and S1A). These findings suggest that the immortalization procedure did not induce detectable chromosomal abnormalities in the endometriosis-derived epithelial cells.

By contrast, immortalized cells derived from the teratoma lesion (iEn2) displayed heterogeneous karyotypic patterns

Table II. Karyotype pattern distribution observed in iEn2 cells.

Pattern	Number of metaphase cells	Fraction of total, %
46,XX (normal karyotype)	13	33.3
46,XX with abnormalities	10	25.6
45,XX with abnormalities	8	20.5
44,XX with abnormalities	4	10.3[a]
42,XX with abnormalities	1	2.6
41,XX with abnormalities	1	2.6
46,X,-X with abnormalities	1	2.6
41,X,-X with abnormalities	1	2.6
Total	39	100.1[a]

[a]Percentages may not sum to exactly 100.0% due to independent rounding of individual values.

Table III. Common defined recurrent cytogenetic abnormality pattern found in iEn2 cells.

Cytogenetic abnormality	Number of metaphase cells	Recurrent cytogenetic abnormality, %
Add(11)(p15)	13	26.0
Add(17)(q25)	4	8.0
Add(12)(q24.3)	3	6.0
Monosomy 11	6	12.0
Monosomy 17	5	10.0
Monosomy 13	4	8.0
Monosomy 5	3	6.0
Monosomy X	2	4.0
Monosomy 4	2	4.0
Monosomy 7	2	4.0
Monosomy 12	2	4.0
Monosomy 18	2	4.0
Monosomy 20	2	4.0
Total	50	100.0

characterized by both numerical and structural chromosomal abnormalities (Figs. 3B and S1B). The composite karyotype was described as 41~46,XX,-X,-4,-5,-7,-11,add(11)(p15),-12,add(12)(q24.3),-13,-17,add(17)(q25),-18,-20,+15mar[cp24]/46,XX[13]. The modal chromosome number was 46,XX, observed in 13 of 39 metaphase cells (33.3%), indicating the presence of a cytogenetically normal subpopulation. The remaining cells demonstrated various abnormal karyotypic patterns including: i) 46,XX with structural rearrangement; ii) 45,XX; iii) 44,XX; iv) 42,XX; v) 41,XX; vi) 46,X,-X; and vii) 41,X,-X modal patterns (Table II). The common defined recurrent cytogenetic abnormality pattern included 50 abnormalities among 39 metaphase cell analyses. Recurrent defined structural cytogenetic abnormalities most frequently involved chromosome 11, particularly add(11)(p15) (13/50 recurrent cytogenetic abnormalities, 26.0%), add(17)(q25) (4/50 recurrent cytogenetic abnormalities, 8.0%) and add(12)(q24.3) (3/50 recurrent cytogenetic abnormalities, 6.0%). Recurrent defined numerical cytogenetic abnormalities involved monosomy 11 (6/50, 12.0%), monosomy 17 (5/50, 10.0%), monosomy 13 (4/50, 8.0%), monosomy 5 (3/50, 6.0%) and monosomy X, 4, 7, 12, 18 and 20 (2/50, 4.0% each) (Table III). Marker chromosomes were identified in multiple abnormal metaphases, contributing to karyotypic complexity and substantial cytogenetic heterogeneity within the cell population.

These findings indicate that the two immortalized epithelial cell lines displayed markedly different genomic characteristics despite undergoing identical immortalization procedures. The endometriosis-derived line maintained chromosomal stability, whereas the teratoma-derived line exhibited intrinsic chromosomal instability consistent with its germ-cell tumor origin (16).

In vivo lesion-forming capacity of endometriosis-derived immortalized cells. To assess whether immortalized endometriosis-derived epithelial cells retain disease-relevant biological properties *in vivo*, iEn1 cells were evaluated

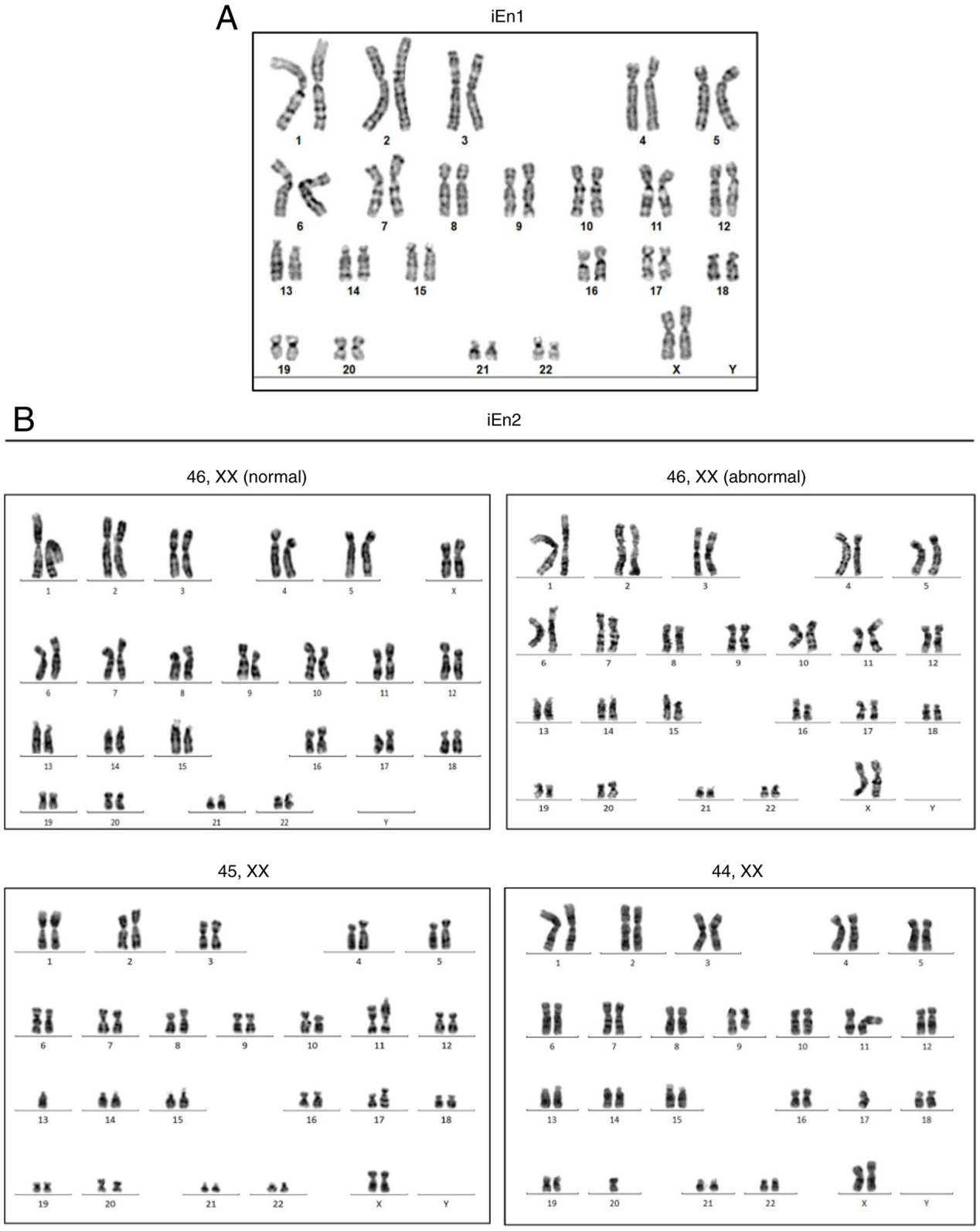

Figure 3. Cytogenetic characterization of immortalized ovarian epithelial cell lines. Representative G-banded karyotypes of immortalized cell lines. (A) iEn1 cells exhibited a normal female karyotype (46,XX), indicating chromosomal stability following immortalization. (B) iEn2 cells demonstrated near-diploid to diploid karyotypes with numerical and structural chromosomal abnormalities, including recurrent losses and structural additions. Representative normal (46,XX) and abnormal (45,XX,-13; 44,XX,-17,-20) karyotypes are shown, illustrating clonal heterogeneity consistent with the pathology-associated genomic instability.

using an estrogen-supplemented xenograft mouse model. Ovariectomized BRJ mice received intraperitoneal implantation of iEn1 cells under estradiol supplementation. A total of 20 days after implantation, histological examination of peritoneal tissues revealed the presence of microscopic glandular structures in mice receiving iEn1 cells at both implantation

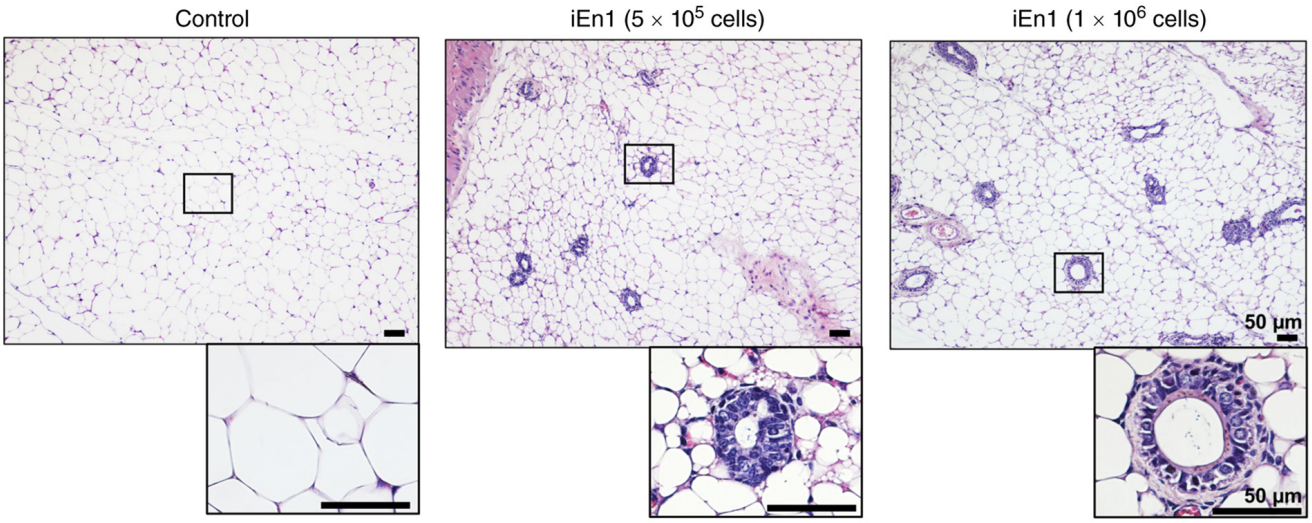

Figure 4. *In vivo* lesion-forming capacity of endometriosis-derived immortalized cells under estrogenic conditions. Ovariectomized BRJ mice received intraperitoneal implantation of iEn1 cells under estrogen supplementation (n=2 per group). The control mice received only the vehicle. Histological evaluation using H&E staining at day 20 post-implantation revealed microscopic glandular structures consistent with endometriosis-like lesions in the iEn1-treated groups ($5x10^5$ and $1x10^6$ cells), whereas no comparable lesions were observed in the controls. Scale bar, 50 μm.

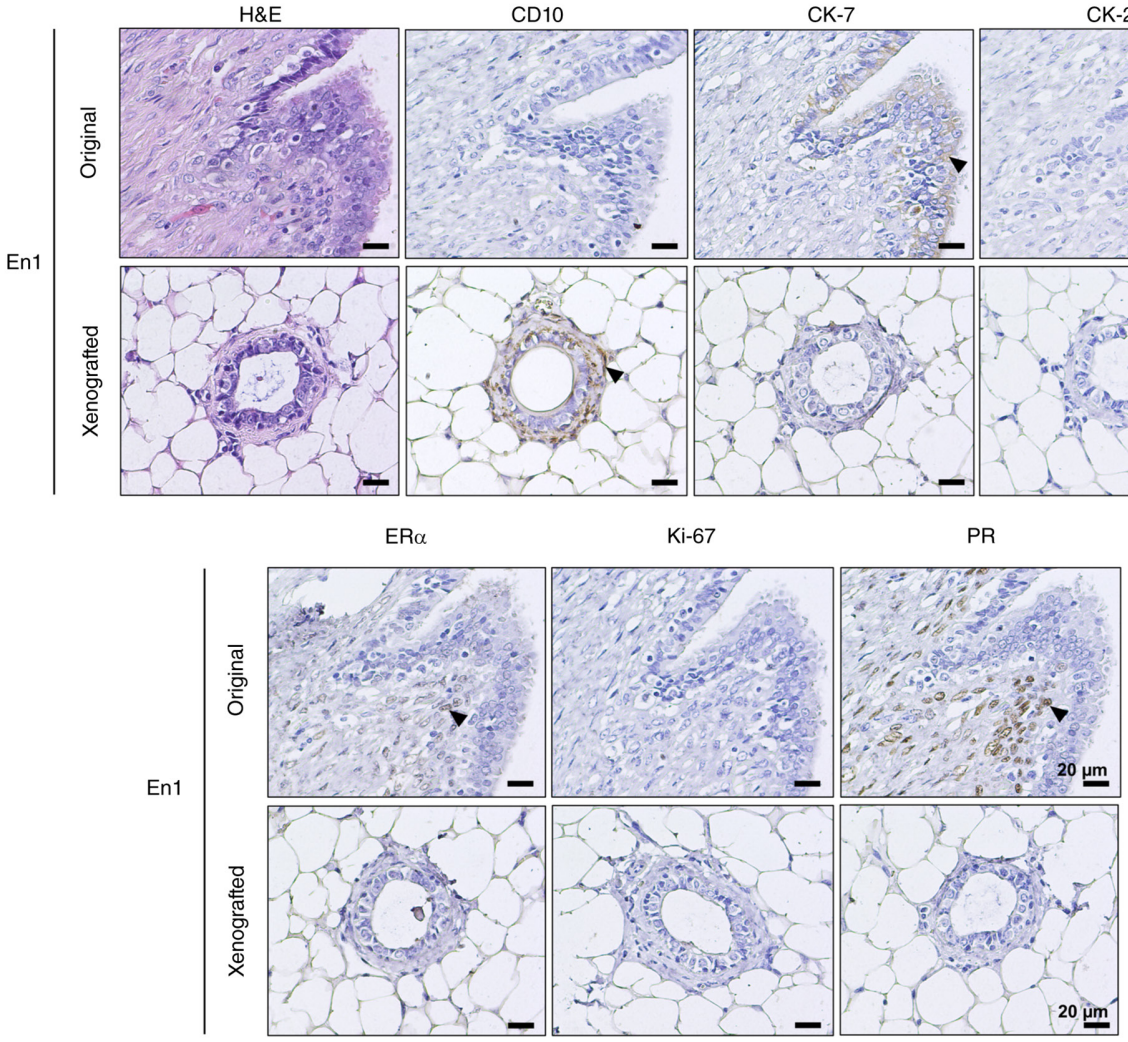

Figure 5. Immunohistochemical comparison of original endometriotic tissue and iEn1-derived xenograft lesions. Representative immunohistochemical staining for CD10, CK-7, CK-20, ERα, PR and Ki-67 in original patient tissue and iEn1-derived xenograft lesions. The expression patterns of epithelial markers and hormone receptor in the original tissues are consistent with endometriosis. Xenografted tissues exhibited partial preservation of marker expression within the murine microenvironment. H&E staining is shown for histological comparison. Scale bar, 20 μm. CK, cytokeratin; ER, estrogen receptor; PR, progesterone receptor.

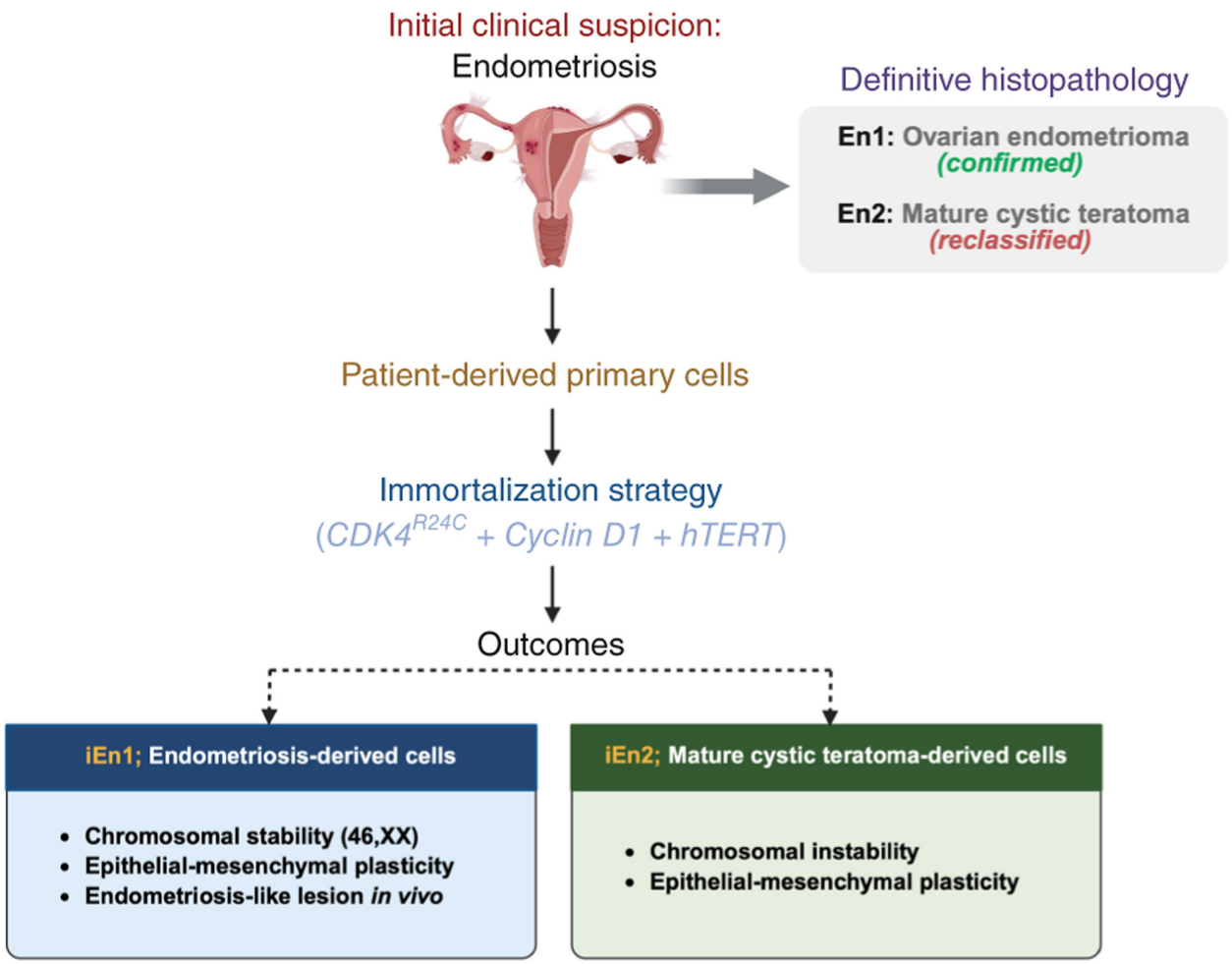

Figure 6. Schematic overview of the establishment and validation of a patient-derived immortalized epithelial model of ovarian endometriosis. Primary epithelial cells isolated from ovarian cystic lesions were immortalized using lentiviral co-expression of $CDK4^{R24C}$, cyclin D1 and hTERT, followed by histopathological stratification and biological characterization to generate a disease-relevant endometriotic epithelial cell model. The endometriosis-derived cell line (iEn1) retained a normal karyotype, whereas the second immortalized line (iEn2) exhibited chromosomal instability consistent with its teratoma-derived origin. CDK4, cyclin-dependent kinase 4; hTERT, human telomerase reverse transcriptase.

doses ($5x10^5$ and $1x10^6$ cells). By contrast, no comparable structures were observed in control animals (Fig. 4). These glandular formations exhibited morphological features consistent with endometriosis-like lesions.

Histopathological comparison between xenografted lesions and the original patient tissues revealed a comparable glandular architecture. Immunohistochemical staining further demonstrated positive expression of CK-7, ERα and PR, which were also robustly expressed in the original tissues, and negative expression of CK-20 (Fig. 5). Furthermore, CD10 was detected in the stromal components of the xenografted lesions, and Ki-67 indicated low proliferative activity. Although marker expression patterns were partially preserved within the BRJ microenvironment, the overall histological features described above supported the capacity of iEn1 cells to generate endometriosis-like glandular structures under estrogenic conditions.

To further evaluate whether xenografted lesions preserve additional endometriosis-associated molecular features, immunohistochemical staining was performed for ERβ (ESR2) and IL-6, whose levels are frequently reported to be elevated in endometriotic lesions (17,18). Unlike the results of ERα staining shown in Fig. 5, IL-6 staining was negative in the epithelial component of both the original patient tissue and the iEn1-derived xenograft, whereas ERβ exhibited occasional positive staining in a few cells of the original tissue but was negative in the xenografts (Fig. S2), indicating that this absence reflects an intrinsic feature of the parental tissue rather than an artifact of immortalization or xenografting. To further evaluate the direct *in vitro* functional responsiveness of the immortalized cells to estrogen, iEn1 and iEn2 cells were treated with β-estradiol. Over the short period tested, β-estradiol treatment failed to induce cell proliferation (Fig. S3A) or upregulate the mRNA expression of key inflammatory mediators, including *COX-2* and *IL-6* (Fig. S3B), in either cell line.

Owing to the limited number of experimental animals (n=2 per group), quantitative assessment of the lesion burden was not performed. Therefore, the xenograft findings are presented as descriptive evidence supporting the lesion-forming capacity of the immortalized endometriosis-derived epithelial cells. Moreover, to avoid confounding the biological interpretation, teratoma-derived iEn2 cells were not evaluated in the xenograft model because they do not represent endometriosis-specific pathology.

Discussion

The present study established and characterized an immortalized epithelial cell model derived from ovarian endometrioma using co-expression of $CDK4^{R24C}$, cyclin D1 and hTERT. The resulting cell line, iEn1, demonstrated sustained proliferative capacity, preservation of epithelial lineage markers and chromosomal stability following immortalization. Furthermore, these cells retained epithelial-mesenchymal plasticity and generated microscopic endometriosis-like glandular structures in an estrogen-supplemented xenograft model. Together, these findings indicate that immortalization using the $CDK4^{R24C}$-cyclin D1-hTERT strategy can support the development of long-term experimental epithelial models while preserving key structural and phenotypic features relevant to endometriosis. The overall rationale and workflow of the present study are summarized in Fig. 6.

The establishment of reliable cellular models remains a major challenge in endometriosis research (5). Although primary epithelial cells derived from patient lesions preserve disease-specific biological characteristics, their limited proliferative lifespan restricts their use for mechanistic studies and long-term experimental manipulation (6,7). Immortalization strategies provide a potential solution to this limitation; however, concerns remain that genetic manipulation may introduce chromosomal instability or alter intrinsic cellular behavior (9,10,19-21). Consistent with a previous report describing the immortalization of human cells using $CDK4^{R24C}$ and cyclin D1 in combination with telomerase activation (10), the immortalized endometriosis-derived epithelial cells in the present study retained a stable karyotype and maintained epithelial lineage characteristics. Therefore, the immortalization strategy used here can extend cellular lifespan without inducing overt genomic instability in epithelial cells derived from benign gynecological tissue. Regarding the baseline expression of CDK4, primary endometriotic epithelial cells exhibited detectable endogenous CDK4 levels prior to transduction. Consequently, the elevated CDK4 signals observed in the immortalized lines should be interpreted as a combination of baseline cellular expression and exogenous lentiviral-driven expression.

Epithelial-mesenchymal plasticity is an important biological feature observed in immortalized epithelial cell lines. Both immortalized lines expressed epithelial markers together with mesenchymal-associated proteins, including vimentin and N-cadherin (22,23). To further confirm the epithelial identity and distinguish iEn1 and iEn2 cells from stromal contaminants, expression of epithelial junction-associated proteins, including β-catenin and claudin-1, was demonstrated. Increasing evidence indicates that partial epithelial-to-mesenchymal transition represents a characteristic feature of endometriotic epithelial cells and contributes to the ability of lesions to implant and persist at ectopic sites (3,4). The preservation of this hybrid epithelial-mesenchymal phenotype in iEn1 cells suggests that the immortalization procedure did not fundamentally disrupt intrinsic cellular programs associated with endometriosis biology. Similarly, baseline vimentin expression was detectable in primary epithelial cells prior to immortalization. The presence of vimentin before transduction reflects the intrinsic epithelial-mesenchymal plasticity characteristic of primary endometriotic epithelial cells, confirming that this hybrid phenotype is an inherent biological feature rather than an artifact induced by the immortalization process.

Notably, cytogenetic analysis and STR profiling revealed marked differences between the two immortalized epithelial cell lines, despite the identical immortalization procedures. STR authentication conclusively verified the independent patient origins of iEn1 and iEn2, precluding cross-contamination artifacts, which are a persistent issue in long-term cell cultures. The endometriosis-derived line (iEn1) retained a normal female karyotype, whereas the second immortalized line (iEn2) demonstrated substantial chromosomal instability characterized by numerical and structural abnormalities. Because both cell lines underwent the same immortalization protocol, these observations strongly suggest that the divergent genomic characteristics primarily reflect the intrinsic properties of the originating tissue rather than artifacts introduced during immortalization.

Postoperative histopathological analysis provided critical insights into the origin of these differences. Although both lesions were clinically suspected to represent ovarian endometriomas, definitive pathological examination revealed that the second lesion represented a mature cystic teratoma. Mature cystic teratomas originate from germ cells and frequently exhibit genomic complexity and chromosomal instability, consistent with the cytogenetic findings observed in iEn2 cells (16,24). These results highlight the importance of integrating pathological diagnosis with experimental characterization when interpreting the biological properties of patient-derived cellular models.

Functional evaluation using an estrogen-supplemented xenograft model further supported the biological relevance of immortalized endometriosis-derived epithelial cells. Following intraperitoneal implantation, iEn1 cells generated microscopic glandular structures resembling endometriosis-like lesions within the peritoneal cavity. Histological comparison between xenografted lesions and the original patient tissue demonstrated similar glandular architecture, and immunohistochemical staining revealed partial preservation of epithelial and hormone receptor expression patterns. Although the number of experimental animals was limited and the findings should therefore be interpreted as descriptive, these observations suggest that immortalized endometriosis-derived epithelial cells can retain disease-relevant functional characteristics *in vivo* (5).

A critical difference between iEn1 and previously published models is the relative lack of direct *in vitro* signaling response. In the current study, β-estradiol treatment failed to induce proliferation or upregulate key inflammatory mediators, such as *COX-2* and *IL-6*, in iEn1 or iEn2 cells over the short period tested. Consistent with this reduced *in vitro* hormonal responsiveness, ERβ or IL-6 expression was not detected in immunohistochemical analysis of the original patient tissue and the corresponding xenografted lesion, in contrast to the ERα positivity observed within the same lesions. Rather than reflecting a technical artifact of immortalization or xenografting, this convergent absence at both the transcript (*COX-2*/*IL-6* mRNA) and

protein (ERβ/IL-6) levels suggests that hormone-driven inflammatory signaling, a feature commonly reported in endometriotic lesions (17,18), may not be a dominant pathway in this particular patient-derived model, reflecting inter-patient heterogeneity in disease biology. This lack of acute estrogenic responsiveness in culture, when contrasted with the *in vivo* data, raises the possibility that proliferative maintenance of the established iEn1 line is less dependent on acute estrogen stimulation and may be influenced by immortalization-associated cell-cycle support. Alternatively, endometriotic epithelial cells *in vivo* may depend on paracrine signaling from stromal and immune cell populations that are absent in isolated 2D epithelial cultures, which may account for the discrepancy between the mild *in vitro* response and the estrogen-dependent glandular formation observed *in vivo*. Collectively, these findings suggest that immortalization alone does not define the biological validity of patient-derived cellular models. Instead, the intrinsic biological properties of immortalized cells remain strongly influenced by the tissue from which they originate. The comparison between iEn1 and iEn2 cells illustrates how two epithelial cultures subjected to identical immortalization procedures can exhibit markedly different genomic and biological behaviors when derived from distinct pathological entities.

Some limitations of the present study should be acknowledged. First, the number of patient-derived samples was limited, and additional models from independent patients are required to validate further the biological consistency of immortalized endometriosis epithelial cell lines. Second, the *in vivo* xenograft experiments were performed with a small number of animals and were primarily designed to assess the lesion-forming capacity rather than the quantitative disease progression. Third, while glandular self-assembly *in vivo* demonstrates inherent tissue-remodeling capability, the early exhaustion of primary tissue precludes direct side-by-side *in vitro* functional comparisons of migration and invasion capacity. Future studies incorporating larger cohorts and additional functional analyses are necessary to define the biological potential of these immortalized epithelial models fully.

Nonetheless, the present study established a patient-derived immortalized epithelial cell model of ovarian endometriosis and provided experimental evidence supporting its biological relevance. The characterized iEn1 model provides a practical platform for investigating epithelial biology and plasticity in endometriosis and may be useful for selected mechanistic and preclinical applications when interpreted within the limitations of its *in vitro* hormonal responsiveness. These models may provide valuable tools for investigating the molecular mechanisms underlying endometriosis pathogenesis and evaluating potential therapeutic interventions. These findings underscore the importance of careful pathological validation when developing patient-derived cellular models for diseases with diagnostic heterogeneity.

Acknowledgements

Not applicable.

Funding

This work was supported by the Fundamental Fund of the Khon Kaen University, Thailand (to KV) and a scholarship (to NSrik) by the Cho-Kalaphruek Excellent Research Project for Medical Students, Faculty of Medicine, Khon Kaen University, Thailand.

Availability of data and materials

The data generated in the present study may be requested from the corresponding author.

Authors' contributions

SS was involved in conceptualization, methodology, validation of all results, formal analysis, investigation, writing the original draft and visualization of all results. NSrik was involved in conceptualization, methodology, result validation, formal analysis, investigation and visualization of all results. JP was involved in result validation and investigation. PK was involved in formal analysis, data curation and supervision. SA was involved in sample preparation, providing resources and supervision. RD, PW, NSrid, RT and SP were involved in formal analysis and investigation. BC, SO, RT and SP were involved in conceptualization, providing resources and supervision. WS and TE were involved in conceptualization and supervision. KV was involved in conceptualization, methodology, result validation, formal analysis, investigation, writing the original draft, reviewing and editing, result visualization, project administration and funding acquisition. SS, NSrik and KV confirm the authenticity of all the raw data. All authors read and approved the final manuscript.

Ethics approval and consent to participate

The present study was approved by the Human Research Ethics Committee of Khon Kaen University (approval nos. HE661409 and HE681046) and conducted in accordance with The Declaration of Helsinki. Written informed consent was obtained from all participants, including the left-over specimen from another project (approval no. HE651590). All animal procedures were approved by the Institutional Animal Care and Use Committee of Khon Kaen University (approval no. IACUC-KKU14/68) and complied with the ARRIVE guidelines.

Patient consent for publication

Not applicable.

Competing interests

The authors declare that they have no competing interests.

Use of artificial intelligence tools

During the preparation of this work, AI tools (Claude; Anthropic PBC) were used to improve the readability and language of the manuscript or to generate images, and subsequently, the

authors revised and edited the content produced by the AI tools as necessary, taking full responsibility for the ultimate content of the present manuscript.

References

1. Giudice LC and Kao LC: Endometriosis. Lancet 364: 1789-1799, 2004.
2. Burney RO and Giudice LC: Pathogenesis and pathophysiology of endometriosis. Fertil Steril 98: 511-519, 2012.
3. Hosseinirad H, Jeong JW and Barrier BF: Insights into the molecular mechanisms and signaling pathways of epithelial to mesenchymal transition (EMT) in the pathophysiology of endometriosis. Int J Mol Sci 26: 7460, 2025.
4. Ma L, Andrieu T, McKinnon B, Duempelmann L, Peng RW, Wotzkow C, Müller C and Mueller MD: Epithelial-to-mesenchymal transition contributes to the downregulation of progesterone receptor expression in endometriosis lesions. J Steroid Biochem Mol Biol 212: 105943, 2021.
5. Black V, Bafligil C, Greaves E, Zondervan KT, Becker CM and Hellner K: Modelling endometriosis using in vitro and in vivo systems. Int J Mol Sci 26: 580, 2025.
6. Kyo S, Nakamura M, Kiyono T, Maida Y, Kanaya T, Tanaka M, Yatabe N and Inoue M: Successful immortalization of endometrial glandular cells with normal structural and functional characteristics. Am J Pathol 163: 2259-2269, 2003.
7. Son D, Park H, An G, Park S, Hwang DW, Park SJ, Kim HS, Lim W, You S and Song G: Establishment of immortalized human endometriotic stromal cell line from ectopic lesion of a patient with endometriosis. Reprod Sci 30: 2703-2714, 2023.
8. Yaswen P, MacKenzie KL, Keith WN, Hentosh P, Rodier F, Zhu J, Firestone GL, Matheu A, Carnero A, Bilsland A, *et al*: Therapeutic targeting of replicative immortality. Semin Cancer Biol 35 (Suppl): S104-S128, 2015.
9. Kiyono T, Foster SA, Koop JI, McDougall JK, Galloway DA and Klingelhutz AJ: Both Rb/p16INK4a inactivation and telomerase activity are required to immortalize human epithelial cells. Nature 396: 84-88, 1998.
10. Shiomi K, Kiyono T, Okamura K, Uezumi M, Goto Y, Yasumoto S, Shimizu S and Hashimoto N: CDK4 and cyclin D1 allow human myogenic cells to recapture growth property without compromising differentiation potential. Gene Ther 18: 857-866, 2011.
11. Hansen KA and Eyster KM: Genetics and genomics of endometriosis. Clin Obstet Gynecol 53: 403-412, 2010.
12. Laganà AS, Garzon S, Götte M, Viganò P, Franchi M, Ghezzi F and Martin DC: The pathogenesis of endometriosis: Molecular and cell biology insights. Int J Mol Sci 20: 5615, 2019.
13. Sasaki R, Narisawa-Saito M, Yugawa T, Fujita M, Tashiro H, Katabuchi H and Kiyono T: Oncogenic transformation of human ovarian surface epithelial cells with defined cellular oncogenes. Carcinogenesis 30: 423-431, 2009.
14. Livak KJ and Schmittgen TD: Analysis of relative gene expression data using real-time quantitative PCR and the 2(-Delta Delta C(T)) method. Methods 25: 402-408, 2001.
15. Zeitvogel A, Baumann R and Starzinski-Powitz A: Identification of an invasive, N-cadherin-expressing epithelial cell type in endometriosis using a new cell culture model. Am J Pathol 159: 1839-1852, 2001.
16. Harms D, Zahn S, Göbel U and Schneider DT: Pathology and molecular biology of teratomas in childhood and adolescence. Klin Padiatr 218: 296-302, 2006.
17. De Andrade VT, Nácul AP, Dos Santos BR, Lecke SB, Spritzer PM and Morsch DM: Circulating and peritoneal fluid interleukin-6 levels and gene expression in pelvic endometriosis. Exp Ther Med 14: 2317-2322, 2017.
18. Han SJ, Jung SY, Wu SP, Hawkins SM, Park MJ, Kyo S, Qin J, Lydon JP, Tsai SY, Tsai MJ, *et al*: Estrogen receptor beta modulates apoptosis complexes and the inflammasome to drive the pathogenesis of endometriosis. Cell 163: 960-974, 2015.
19. Muraoka A, Osuka S, Kiyono T, Suzuki M, Yokoi A, Murase T, Nishino K, Niimi K, Nakamura T, Goto M, *et al*: Establishment and characterization of cell lines from human endometrial epithelial and mesenchymal cells from patients with endometriosis. F S Sci 1: 195-205, 2020.
20. Fang J, Yang Y, Xiao Y and Lü P: The evolution of endometriosis research models: A paradigm shift from immortalized cell lines to organoids. Biol Reprod 114: 1186-1198, 2026.
21. Sohel HI, Kiyono T, Zahan UF, Razia S, Ishikawa M, Yamashita H, Kanno K, Sonia SB, Nakayama K and Kyo S: Establishment of a novel in vitro and in vivo model to understand molecular carcinogenesis of endometriosis-related ovarian neoplasms. Int J Mol Sci 26: 1995, 2025.
22. Konrad L, Dietze R, Riaz MA, Scheiner-Bobis G, Behnke J, Horné F, Hoerscher A, Reising C and Meinhold-Heerlein I: Epithelial-mesenchymal transition in endometriosis-when does it happen? J Clin Med 9: 1915, 2020.
23. Matsuzaki S and Darcha C: Epithelial to mesenchymal transition-like and mesenchymal to epithelial transition-like processes might be involved in the pathogenesis of pelvic endometriosis. Hum Reprod 27: 712-721, 2012.
24. Suda K, Nakaoka H, Yoshihara K, Ishiguro T, Tamura R, Mori Y, Yamawaki K, Adachi S, Takahashi T, Kase H, *et al*: Clonal expansion and diversification of cancer-associated mutations in endometriosis and normal endometrium. Cell Rep 24: 1777-1789, 2018.